Sorption and breathing properties of difluorinated MIL-47 and Al-MIL-53 frameworks

Shyam Biswas [a], Sarah Couck [b], Dmytro Denysenko [c], Asamanjoy Bhunia [d], Maciej Grzywa [c], Joeri F.M. Denayer [b], Dirk Volkmer [c], Christoph Janiak [d], Pascal Van Der Voort [a,*]

[a] Dept. of Inorganic and Physical Chemistry, Centre for Ordered Materials, Organometallics and Catalysis, Ghent University, Krijgslaan 281-S3, 9000 Ghent, Belgium
[b] Department of Chemical Engineering, Vrije Universiteit Brussel, Pleinlaan 2, 1050 Brussel, Belgium
[c] Institute of Physics, Chair of Solid State and Material Science, Augsburg University, Universitätsstrasse 1, 86135 Augsburg, Germany
[d] Institut für Anorganische Chemie und Strukturchemie, Universität Düsseldorf, Universitätsstraße 1, 40225 Düsseldorf, Germany

1. Introduction

Metal–organic frameworks (MOFs) [1–3], which are a relatively new class of nanoporous materials, have received significant attention due to their exceptionally high porosities and chemically tunable structures leading to potential applications in a wide range of areas including gas storage/separation [4–6], catalysis [7,8] and drug delivery [9–12]. The pore dimensions or surface property of MOFs can be sytematically varied by attaching functional groups having diverse properties to the organic linker, which is impossible with zeolites. The functionalization does not affect the inherent topology of the framework. The functionalization of both rigid and flexible (often denoted as "breathing" [13]) MOFs can be accomplised (i) by using pre-functionalized linkers during synthesis or (ii) by a post-synthetic modification strategy[14]. The functionalization of rigid MOFs influences their sorption [15–21], selectivity [22,23], thermal and chemical stability [24]. Moreover, the breathing property of flexible MOFs can be affected due to functionalization [25–29].

The terephalate based MOFs MIL-47(V^{IV}) [30] (MIL = Material of the Institut Lavoisier) and Al-MIL-53 [31] are well-studied because of their various potential applications [1]. They have the general composition [M(X)(BDC] (X = OH, M = Al^{III} for Al-MIL-53 and X = O, M = V^{IV} for MIL-47(V^{IV}); BDC = 1,4-benzenedicarboxylate). Their frameworks consist of infinite *trans* chains of corner-sharing [$V^{IV}O_6$] or [$Al^{III}O_4(OH)_2$] octahedra cross-linked by BDC linkers, resulting in a one-dimensional rhombic-shaped channel system (Fig. 1). Upon adsorption of guest molecules, the frameworks of Al-MIL-53 and MIL-47(V^{IV}) show flexibility or rigidity, respectively, which is often ascribed to the presence or absence of μ_2-OH groups in the frameworks. The structural flexibility of Al-MIL-53 is strongly dependent on the size and functionality of the linker molecules, temperature, adsorbate pressure and the nature of the guest molecules [25,29,31]. Hence, the breathing behaviour of Al-MIL-53 have been probed in detail with different guest molecules such as CO_2 [32–37] and linear alkanes [38–43]. For Al-MIL-53, the structural transition occurs between a narrow pore (NP) and

* Corresponding author. Tel.: +32 92644442; fax: +32 92644983.
E-mail address: pascal.vandervoort@ugent.be (P. Van Der Voort).

a large pore (LP) form (cf. Fig. 1) and the reversible transition between the two forms can result in a change in unit cell volume up to 40% [26]. Recently, high mechanical pressure has been applied to induce a LP → NP transition in MIL-47(V^{IV}), which is otherwise rigid [44].

Hydrophobic MOFs have been obtained formerly through functionalization of the frameworks by water-repellent groups such as –F, $–CH_3$, $–CF_3$, $–OCF_3$, etc. [45–50]. The hydrophobic pore surfaces of MOFs facilitates in enhancing the adsorption capacity for hydrocarbons, as shown previously for a Ag(I)-based MOF with the pore walls decorated by $–CF_3$ groups [47]. However, the examples of functionalized hydrophobic MOFs are relatively rare in literature [45–50].

Because of their light weight, non-toxicity and increased stability against moisture [51–53], a broad variety of functionalized Al-MIL-53-X (X = $–NH_2$, –OH, $–CO_2H$, $–(CO_2H)_2$, $–C_6H_4$, –Cl, –Br, $–CH_3$, $–NO_2$, $–(OH)_2$) [25,37,54–59] compounds have been documented. In contrast, MIL-47 is moisture sensitive, although it exhibits significant adsorption capacity for linear hydrocarbons [41–43].

The benefits of hydrophobic MOFs, and those of Al- and V-based MOFs, have provoked us to study the effect of fluorination on the sorption and breathing behaviour of difluorinated MIL-47 and Al-MIL-53 frameworks. It is noteworthy that we have previously carried out similar investigations on monofluorinated MIL-47 and Al-MIL-53 compounds [29].

2. Experimental

2.1. Materials and general methods

The H_2BDC-F_2 ligand was synthesized following a previously reported procedure [60] and its purity was examined by proton nuclear magnetic resonance spectroscopy (NMR) [61] spectroscopy (Fig. S1, Supporting Information). All other starting materials were of reagent grade and used as received from the commercial supplier. Weighing of VCl_3 was performed in a nitrogen-filled glove box. The thermally activated MIL-47-F_2 (**1**) was stored in a glove box owing to its air-sensitivity. All other manipulations were carried out under an air atmosphere. Diffuse-reflectance infrared Fourier transform (DRIFT) spectra were collected with a Thermo Nicolet 6700 FTIR spectrometer equipped with a nitrogen-cooled MCT detector and a KBr beam splitter. The DRIFT cell was connected to a vacuum manifold. The following indications are used to characterize absorption bands: very strong (vs), strong (s), medium (m), weak (w), shoulder (sh), and broad (br). Elemental analyses (C, H, N) were performed with a Thermo Scientific Flash 2000 CHNS-O analyzer equipped with a TCD detector. Thermogravimetric analysis (TGA) was carried out with a Netzsch STA-409CD thermal analyzer in a temperature range of 25–600 °C under an air atmosphere at a heating rate of 2 °C min^{-1}. Ambient temperature X-ray powder diffraction (XRPD) patterns were recorded with a Thermo Scientific ARL X'Tra diffractometer operated at 40 kV, 40 mA with Cu-$K\alpha$ (λ = 1.5406 Å) radiation. Temperature-dependent XRPD patterns of **2** were collected with a Bruker D8 Discover X-ray diffractometer equipped with a linear detector; the XRD patterns were recorded from room temperature to 700 °C with a temperature ramp of 0.1 °C s^{-1} in air flow. Le Bail fits were performed by using the Jana2006 program [62]. The nitrogen sorption isotherms up to 1 bar were measured by using a Belsorp Mini apparatus at −196 °C. The low pressure carbon dioxide sorption analysis was performed using a Belsorp Max instrument combined with BELCryo system at −78.3 °C. The high-pressure nitrogen and carbon dioxide sorption isotherms at 30 °C were recorded by the gravimetric method on a magnetic suspension balance of Rubotherm GmbH. The vapor phase isotherms of *n*-hexane at 50 °C were measured with the gravimetric method on a microbalance of VTI Corporation. Water sorption isotherms at 20 °C were obtained volumetrically from a Quantachrome Autosorb iQ MP instrument equipped with an all-gas option. Prior to the sorption experiments, the compounds were degassed (**1**: 100 °C, 1 h; **2**: 150 °C, 16 h) under dynamic vacuum.

MIL-47 [30] and Al-MIL-53 [31,41] were synthesized and activated as described previously. The phase-purity of the compounds were confirmed by typical characterization experiments (XRPD, TGA, IR spectroscopy, and sorption analysis).

2.2. Synthesis

$[V(OH)(C_8H_2F_2O_4)]\cdot 0.3(C_8H_4F_2O_4)$ (MIL-47-F_2-AS) (1-AS): A mixture of VCl_3 (100 mg, 0.64 mmol) and H_2BDC-F_2 (129 mg, 0.64 mmol) in 2 mL of water was placed in a Pyrex tube (10 mL). The tube was sealed and heated in a microwave synthesizer (CEM, Discover S) to 170 °C at 150 W, held under these conditions for 30 min with stirring, then cooled to room temperature. The greenish yellow precipitate was collected by filtration, washed with acetone and dried in air. The yield was 125 mg (0.38 mmol, 60%). Elemental analysis calcd. for $C_{9.6}H_{3.8}F_{2.4}O_{5.8}V$ (308.46 g mol^{-1}): C 37.40, H 1.24; found: C 38.30, H 1.52%. DRIFT (KBr, cm^{-1}): 3617 (m), 3081 (w), 2874 (br), 1709 (vs), 1579 (vs), 1499 (m), 1481 (sh), 1430 (vs), 1380 (s), 1300 (s), 1265 (s), 1193 (s), 1109 (w), 918 (vs), 867 (w), 832 (w), 802 (s), 778 (s), 754 (m).

$[Al(OH)(C_8H_2F_2O_4)]\cdot 0.5(C_8H_4F_2O_4)$ (Al-MIL-53-F_2-AS) (2-AS): A mixture of $AlCl_3\cdot 6H_2O$ (0.5 g, 2.07 mmol), H_2BDC-F_2 (0.42 g, 2.07 mmol), and water (25 mL) was placed in a 100 mL Teflon liner, and the resulting mixture was heated in a conventional oven at 210 °C for 24 h and cooled to room temperature. The white precipitate was collected by filtration, washed with acetone and dried in air. The yield was 0.48 g (1.39 mmol, 67%). Elemental analysis calcd. for $C_{12}H_5AlF_3O_7$ (345.14 g mol^{-1}): C 41.75, H 1.46; found: C 41.60, H 1.12%. DRIFT (KBr, cm^{-1}): 3676 (m), 3097 (w), 2877 (br), 1710 (vs), 1628 (s), 1500 (sh), 1491 (s), 1449 (vs), 1385 (s), 1299 (m), 1264 (m), 1201 (s), 1011 (vs), 918 (m), 873 (w), 817 (s), 788 (s), 753 (m), 657 (s).

2.3. Activation of the compounds

Direct heating of **1-AS** at 300 °C for 24 h under dynamic vacuum resulted in the evacuated form of the compound.

A two-step activation protocol was applied for **2-AS**. At first, **2-AS** (0.42 g) was suspended in *N,N'*-dimethylformamide (30 mL) and heated at 155 °C for 24 h in a conventional oven. In the second step, the filtered solid (termed as **2-DMF**) was heated at 300 °C under dynamic vacuum for 24 h and thus the activated form of **2** was obtained.

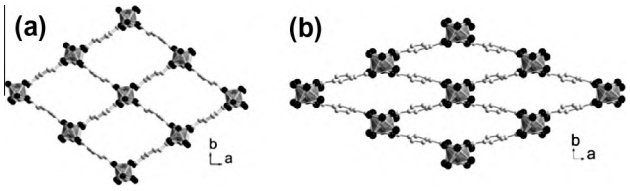

Fig. 1. Ball-and-stick representations of the 3D framework of, (a) large pore (LP), and (b) narrow pore (NP) form of Al-MIL-53 (colour codes: Al, dark gray octahedra, C, light gray; O, black). For clarity, the hydrogen atoms and guest molecules have been omitted from all structural plots. The atomic coordinates provided in Ref. [31] were used to draw the figure.

3. Results and discussion

3.1. Synthesis and activation

Similar to their monofluorinated analogues, **1** and **2** have been synthesized under hydrothermal conditions by using microwave irradiation or electric heating, respectively. The molar ratio of MCl_3 (M = V, **1**; Al, **2**) and $H_2BDC\text{-}F_2$ in the starting aqueous reaction mixtures was 1:1. In sharp contrast to the several days (MIL-47: 4 d, Al-MIL-53: 3 d) of synthesis times required for the pristine solids, **1** and **2** have been synthesized in only 30 min and 1 d, respectively. These synthesis times are similar to MIL-47-F and Al-MIL-53-F [29]. In addition to MIL-47-F, five isostructural and functionalized MIL-47-X (X = $-C_4H_4$, $-(OH)_2$, $-(CH_3)_2$, $-Cl_4$ and $-Br_4$) compounds have been previously synthesized by using microwave irradiation [63].

$H_2BDC\text{-}F_2$ molecules entrapped within the pores of the AS-forms of the compounds were removed by direct thermal treatment (**1-AS**) under vacuum or in a two-step activation procedure (**2-AS**). For **2-AS**, the guest molecules were at first exchanged by heating the AS-form of the compound in a polar solvent such as *N,N′*-dimethylformamide (DMF). In the second step, the guest-exchanged compound was heated under dynamic vacuum for the removal of the DMF molecules. After cooling to room temperature, the thermally activated **2** adsorbs variable amounts of water from air depending on the exposure time.

3.2. DRIFT analysis

The strong absorption bands due to asymmetric and symmetric $-CO_2$ stretching vibrations of the coordinated terephthalate molecules are located in the regions 1565–1631 cm^{-1} and 1429–1449 cm^{-1}, respectively, in the DRIFT spectra (Figs. S2 and S3, Supprting Information) of AS forms of the two compounds [31]. In the DRIFT spectra of AS forms of the compounds, the additional strong absorption bands observed at ca. 1710 cm^{-1} can be attributed to the protonated form ($-CO_2H$) of unreacted or guest $H_2BDC\text{-}F_2$ molecules [31]. In the DRIFT spectra of empty-pore forms of the two compounds, the absorption bands of the guest $H_2BDC\text{-}F_2$ molecules are absent or reduced in intensity, indicating almost complete activation. In the DRIFT spectra of **2-DMF**, a strong absorption band is observed at 1680 cm^{-1}, which can be assigned to the carbonyl stretching vibration of guest DMF molecules. The medium absorption bands in region 3600–3680 cm^{-1} in the DRIFT spectra of **1-AS**, **2-AS**, **2-DMF** and **2** are due to the stretching vibration of the μ_2-OH group [26]. The lack of this absorption band in the DRIFT spectrum of the empty-pore form of **1** indicates the absence of μ_2-OH group in this compound.

3.3. Structure description

Both MIL-47 and Al-MIL-53 (Fig. 1) have the same framework topology. The refined lattice parameters (Table 1) of the different forms of **1** and **2** determined from their ambient temperature XRPD patterns (Figs. S4 and S5, Supporting Information) are similar to the un-functionalized MIL-47 [30] and Al-MIL-53 [31], respectively. Thus, the different forms of **1** and **2** are isostructural with MIL-47 and Al-MIL-53, respectively. Le Bail fits of the XRPD patterns of the various forms of **1** and **2** are presented in Figs. S6–S9, Supporting Information. The 4^4 net of the AS forms of MIL-47 [30] and Al-MIL-53 [31] consists of infinite tilted *trans* chains of corner-sharing (via μ_2-OH group) $[M^{III}O_4(OH)_2]$ (M = V, **1**; Al, **2**) octahedra, which are crosslinked by the carboxylate groups of the BDC linkers. The resulting three-dimensional framework bears one-dimensional (1D) rhombic-shaped channels. The 1D channels of the AS-forms of the difluorinated compounds are occupied by guest $H_2BDC\text{-}F_2$ molecules. The removal of the guest molecules is achieved by thermal activation, which results in the empty-pore forms of the compounds. During thermal activation of **1-AS**, the V^{III} ions are oxidized to V^{IV} and the V–OH bonds are transformed to a vanadyl (V^{IV} = O) group. In contrast, the + 3 oxidation state of the aluminum atoms of **2-AS** remains unaffected during thermal activation. The unit cell volumes (Table 1) of the different forms of **1** and **2** correspond to either large pore (LP) form (crystal system: orthorhombic; unit cell volume: ~1500–1600 $Å^3$) or narrow pore form (crystal system: monoclinic; unit cell volume: ~1200 $Å^3$). Compound **2-DMF** can be classified to the NP form since the c parameter is twice of 6.746 Å and the unit cell volume is twice of 1172.8 $Å^3$ (compare with hydrated forms of **2** and Al-MIL-53).

3.4. Thermal stability

Thermogravimetric analyses (TGA) were performed on the different forms of **1** and **2** in air atmosphere in order to examine their thermal stability. According to the TG analyses, **1** and **2** are thermally stable up to 340 and 480 °C, respectively. The thermal stabilitites of the two difluorinated compounds are comparable to that of un-functionalized MIL-47 (400 °C) or Al-MIL-53 (500 °C). Inspite of bearing the same framework topology, **2** shows higher thermal stability compared to **1**.

In the TG curves of the AS forms of **1** and **2** (Fig. 2), any weight loss step that occurs below the decomposition temperature of the compounds can be ascribed to the removal of the guest $H_2BDC\text{-}F_2$ molecules. The thermally activated form of **2** does not exhibit any weight loss step below the decomposition temperature. This fact suggests that **2** is more hydrophobic as compared to the other known functionalized Al-MIL-53-X (X = –Cl, –Br, $-CH_3$, $-NO_2$, $-NH_2$, $-CO_2H$, $-(OH)_2$) [25,55,59] compounds. Except Al-MIL-53-F [29], the thermally activated forms of the formerly reported

Table 1
Molecular formulae, refined lattice parameters[a] and pore types[b] of the different forms of **1**, **2**, MIL-47 and Al-MIL-53.

Compound	Molecular formula	*a* (Å)	*b* (Å)	*c* (Å)	*V* ($Å^3$)	*β*(deg)	Pore Type
1	$[V^{IV}(OH)(BDC\text{-}F_2)]$	16.612(9)	13.888(7)	6.856(4)	1582(2)		LP
MIL-47 [30]	$[V^{IV}(O)(BDC)]$	16.143(3)	13.939(2)	6.8179(12)	1534.1(5)		LP
2-AS	$[Al(OH)(BDC\text{-}F_2)]\cdot 0.5(H_2BDC\text{-}F_2)$	17.209(4)	12.437(2)	6.693(2)	1432.5(9)		LP
Al-MIL-53-AS [31]	$[Al(OH)(BDC)]\cdot 0.7\ (H_2BDC)$	17.129(2)	12.182(1)	6.628(1)	1383.1(2)		LP
2-DMF	$[Al(OH)(BDC\text{-}F_2)]\cdot 3\ (DMF)$	18.878(4)	9.669(2)	13.493(2)	2345(1)	107.760(5)	NP
Al-MIL-53-DMF [25]	$[Al(OH)(BDC)]\cdot 1.1\ (DMF)$	17.55(6)	11.396(17)	6.615(13)	1322.8(74)		LP
2 (hydrated)[c]	$[Al(OH)(BDC\text{-}F_2)]\cdot x\ H_2O$	19.932(3)	7.095(1)	8.466(1)	1144.1(4)	107.14(1)	NP
Al-MIL-53 (hydrated)[c] [31]	$[Al(OH)(BDC)]\cdot 1.0\ (H_2O)$	19.513(2)	7.612(1)	6.576(1)	946.8(1)	104.24(1)	NP

[a] Lattice parameters were determined from laboratory XRPD data (λ = 1.5406 Å) collected at room temperature.
[b] LP: large pore, NP: narrow pore.
[c] Refers to the forms of **2** and Al-MIL-53 after adsorption of variable amount of water from air when the thermally activated compounds are cooled to room temperature.

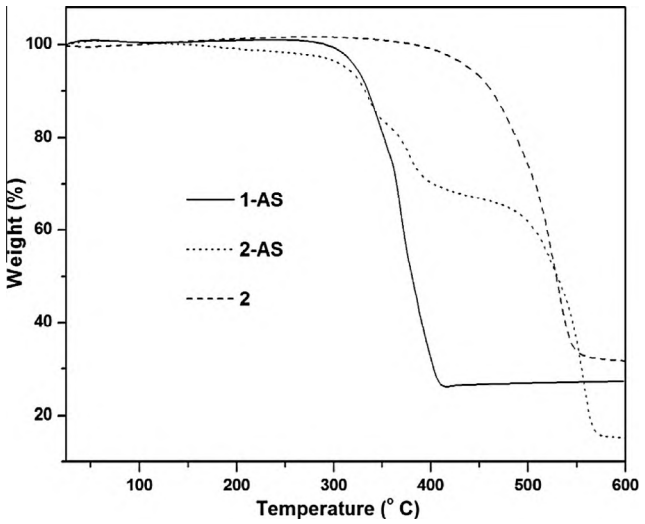

Fig. 2. TG curves of as-synthesized **1** (solid line), as-synthesized **2** (dotted line), and thermally activated **2** (dashed line) recorded in air atmosphere.

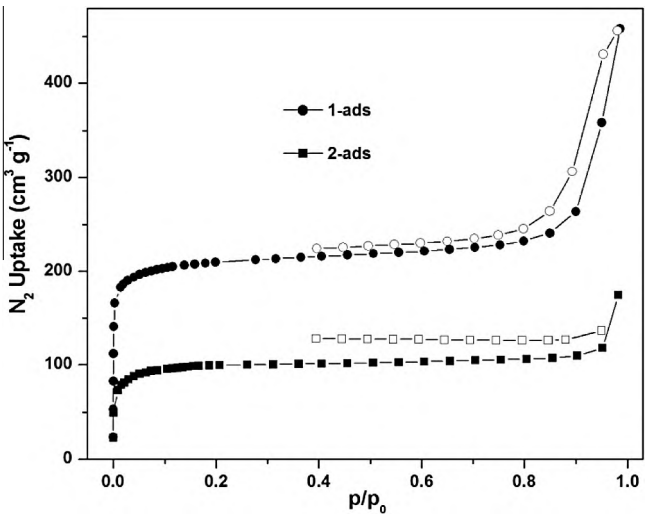

Fig. 3. Low pressure N_2 adsorption (closed symbols) and desorption (open symbols) isotherms of thermally activated **1** (circles) and **2** (squares) recorded at −196 °C.

Al-MIL-53-X compounds were found to adsorb different amounts of water from air depending on the grafted functional groups. Although the weight loss step due to the removal of free H_2BDC-F_2 molecules is not distinct in the TG curve of as-synthesized **1**, their presence in the pores has been verified by DRIFT spectroscopy (Fig. S2, Supporting Information) and elemental analysis. The experimental weight losses for the different forms of **1** and **2** are consistent with the calculated ones as well as the elemental analyses (Tables S1 and S2, Supporting Information). This fact confirms the phase purity of the compounds.

Temperature-dependent XRPD (TDXRPD) experiments were performed on the thermally activated form of **2** in order to explore the possibility of any structural change upon heat treatment. It is obvious from the TDXRPD patterns (Fig. S10, Supporting Information) that no structural transition occurs for the activated form of **2**. Similar phenomenon has formerly been noticed for Al-MIL-53-F [29]. The activated form of **2** is stable up to 660 °C, as gleaned from the TDXRPD patterns. However, the thermal stability obtained from the TDXRPD measurements (6 °C min^{-1}) can not be directly compared with that deduced from the TG analyses (2 °C min^{-1}), since different heating rates have been employed in the two types of experiments.

3.5. Gas/vapor sorption properties

CO_2, *n*-hexane and H_2O sorption experiements were carried out on the thermally activated **1** and **2** in order to examine the influence of the attachment of two –F groups per linker on the sorption and breathing behaviour of the frameworks.

N_2 sorption measurements were performed on the thermally activated **1** and **2** at −196 °C. Type-I adsorption isotherms (Fig. 3) were obtained for both compounds. Table 2 summarizes the micropore volumes derived from the N_2 adsorption isotherms. Both compounds show significant porosity values, which are lower than the ones reported for un-functionalized MIL-47 [30] and Al-MIL-53 [31].

High pressure CO_2 sorption measurements were carried out on the thermally activated **1** and **2** at 30 °C. In both cases, type-I adsorption isotherms (Fig. 4) were obtained. At 30 °C and 22.5 bar, the CO_2 uptake values of **1** and **2** (Table 2) are lower compared to the ones observed for un-modified MIL-47 and Al-MIL-53 at 31 °C and 22.5 bar [37]. Similar to our formerly reported monofluorinated Al-MIL-53 [29], no hysteresis loop was observed in the high pressure CO_2 sorption isotherms of the aluminum-based, difluorinated compound **2**. This behaviour is in sharp contrast to pristine Al-MIL-53 [37]. For the un-functionalized compound, a remarkable hysteresis loop was observed in the high pressure CO_2 adsorption–desorption isotherms at 31 °C [37]. In this way, the attachment of two –F groups per linker in the framework affects the temperature domain for the structrural transition of **2**. Interestingly, **2** shows similar CO_2 uptake capacity as Al-MIL-53-F [29] at 22.5 bar and 30 °C, in spite of a large difference in specific Langmuir surface area (Table 2) between the two compounds. Intrigued by this fact, we measured the high pressure N_2 adsorption isotherm (Fig. 4) of **2** at 30 °C in order to determine the ideal CO_2/N_2 selectivity. From the initial slopes of the single component adsorption isotherms, ideal CO_2/N_2 adsorption selectivity value (determined as ratio of the initial slopes) of 11 was obtained. It is worthy to note that similar or even higher CO_2/N_2 selectivity values have previously been reported for a variety of MOFs [64–75].

Low-pressure CO_2 sorption measurement (Fig. 5) was performed on the thermally activated **2** at −78.3 °C up to 1 bar. The analysis reveals the existence of two hysteresis loops, as previously observed for Al-MIL-53-F [29] in CO_2 sorption isotherms measured at the same temperature and up to 1 bar. The hysteresis loops observed for the difluorinated Al-MIL-53 compound are less pronounced as compared to its monofluorinated analogue and they are only clearly visible when the isotherms are plotted in the semi-logarithmic scale. Similar hysteresis loops have also formerly been found to occur for un-functionalized Al-MIL-53 in CH_4 (−49 °C, up to 6 bar) [32] and Xe (−53 °C, up to 1 bar) [76] sorption isotherms. For Al-MIL-53 (CH_4 and Xe sorption) and Al-MIL-53-F (CO_2 sorption), the occurrence of hysteresis loops in the lower and higher pressure domains of the sorption isotherms under the above mentioned conditions was ascribed to the LP → NP and NP → LP transitions, respectively. Moreover, *in situ* XRPD experiments confirmed such structural transitions in Al-MIL-53-F upon adsorption of CO_2 [29]. Based on these similarities in the shape of sorption isotherms with those of Al-MIL-53 and Al-MIL-53-F, it can be hypothesized that the hysteresis loops in the lower and higher pressure regions in the low pressure CO_2 sorption isotherms of **2** at −78.3 °C are due to the LP → NP and NP → LP transitions, respectively. At −78.3 °C and 1 bar, **2** exhibits a high CO_2 adsorption capacity of 9.8 mmol g^{-1}.

H_2O sorption experiments (Fig. 6) were performed on the thermally activated **1** and **2** at 20 °C in order to investigate the

Table 2
Specific Langmuir surface areas, micropore volumes and CO_2 uptake values of **1**, **2**, MIL-47-F, Al-MIL-53-F, MIL-47 and Al-MIL-53.

Compound	Specific langmuir surface area[a] ($m^2\ g^{-1}$)	Micropore volume[b] ($cm^3\ g^{-1}$)	CO_2 uptake[c] at 22.5 bar (mmol g^{-1})
1	987	0.34	7.0
2	467	0.16	6.9
MIL-47-F	1078 [29]	0.36	6.7 [29]
Al-MIL-53-F	1137 [29]	0.48	7.6 [29]
MIL-47	1222 [29]	0.38	11.5 [37]
Al-MIL-53	1590 [29]	0.55	10.0 [37]

[a] The specific Langmuir surface areas have been calculated from the N_2 adsorption isotherms.
[b] The micropore volumes have been calculated at $p/p_0 = 0.5$.
[c] Except MIL-47 and Al-MIL-53 (31 °C), the CO_2 uptake values have been achieved at 30 °C.

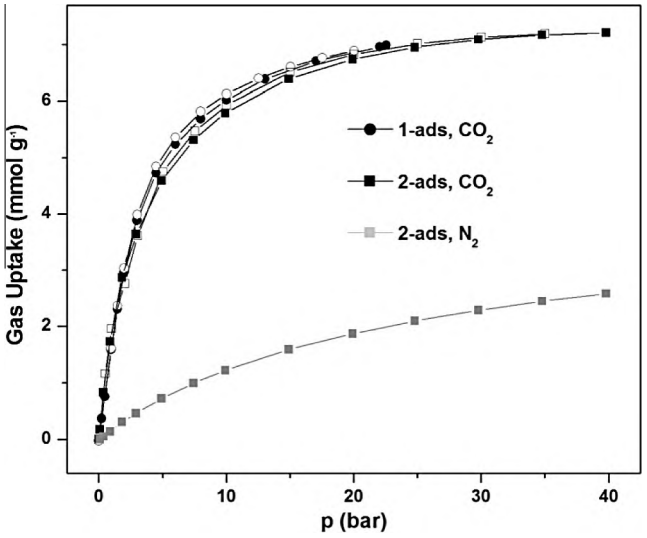

Fig. 4. High pressure CO_2 (black) and N_2 (grey) adsorption (closed symbols) and desorption (open symbols) isotherms of thermally activated **1** (circles) and **2** (squares) measured at 30 °C.

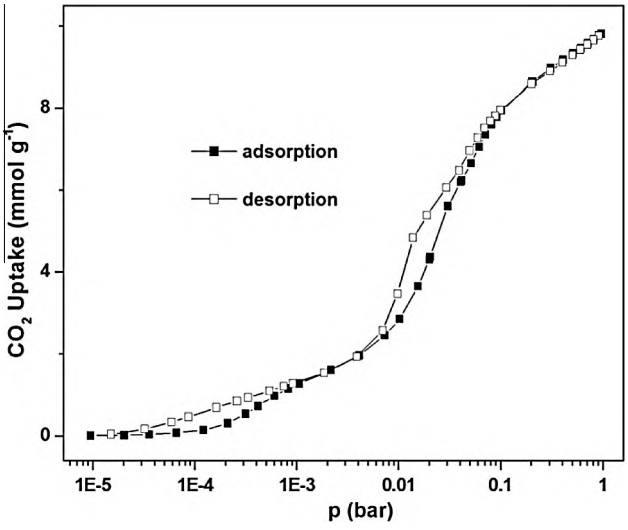

Fig. 5. Low pressure CO_2 adsorption (closed symbols) and desorption (open symbols) isotherms of thermally activated **2** measured at −78.3 °C (semi-logarithmic scale).

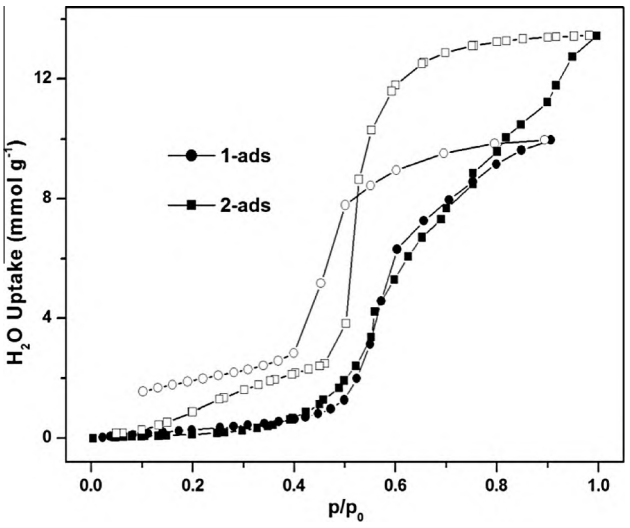

Fig. 6. H_2O adsorption (closed symbols) and desorption (open symbols) isotherms of thermally activated **1** (circles) and **2** (squares) measured at 20 °C.

anticipated hydrophobicity owing to the incorporation of –F groups in the frameworks. Both **1** and **2** show low H_2O uptake value (<1 mmol g^{-1}) below p/p_0 value of 0.5, as expected. Afterwards, an abrupt increase in H_2O uptake capacity is observed for both compounds. At $p/p_0 = 0.9$, the H_2O uptake value of **1** and **2** reaches 9.8 and 11.4 mmol g^{-1}, respectively. The H_2O adsorption in both **1** and **2** follows type-V isotherms [77]. Such isotherms have rarely [29,49,58,78,79] been found in other MOFs. The H_2O adsorption capacity of **2** at $p/p_0 = 0.9$ falls in the range of other (–F, –Cl, –Br, $–CH_3$, $–NO_2$, $–NH_2$: 3.7–7.7 mmol g^{-1}, $–(OH)_2$: 24.3 mmol g^{-1}) [25,29] functionalized Al-MIL-53 compounds. Similar to our previous work on mono-fluorinated MIL-47 and Al-MIL-53 compounds [29], both of the difluorinated compounds presented herein thus exhibit a certain amount of hydrophobicity. However, the extent of hydrophobicity in the presented compounds has not been increased due to the attachment of one extra –F group per linker. Noticeably, highly water-resistant MOFs have formerly been prepared through the introduction of water-repellant –F, $–CH_3$, $–CF_3$ and $–OCF_3$ groups in the frameworks [45–50].

Large adsorption capacity for hydrophobic gas molecule such as *n*-hexane has been formerly observed for parent MIL-47 and Al-MIL-53 [39,41,42]. The inherent hydrophobicity of MIL-47 and the extra hydrophobicity achieved through the incorporation of two –F groups per linker in the frameworks of **1** and **2** inspired us to measure the *n*-hexane sorption isotherms (Fig. 7) of the two compounds at 50 °C. The *n*-hexane adsorption in **1** and **2** follows type-I isotherms. No sub-step is observed in the *n*-hexane sorption isotherm of **2**. This phenomenon is contrary to un-functionalized Al-MIL-53 [41]. In this way, the expected structural change of **2** upon the adsorption of *n*-hexane is suppressed by the grafted –F groups. The *n*-hexane uptake values of **1** and **2** (Table 3) at 50 °C and $p/p_0 = 0.5$ are comparable to those of pristine and monofluorinated MIL-47 and Al-MIL-53 [29,41]. It is obvious from Table 2 that the difference in specific surface area between **2** and Al-MIL-53 is much larger compared to that between **1** and MIL-47. Thus, the increase in hydrophobicity in **1** compensates the decrease in specific surface due to fluorination, leading to higher *n*-hexane uptake value compared to pristine MIL-47. However, the increase in hydrophobicity in **2** fails to compensate the decrease in specific surface area, resulting in lower *n*-hexane adsorption capacity compared to un-functionalized Al-MIL-53. It is worth noting that the *n*-hexane uptake value of **1** and MIL-47-F [29] at 50 °C and $p/p_0 = 0.5$ are same and surpass that of parent MIL-47.

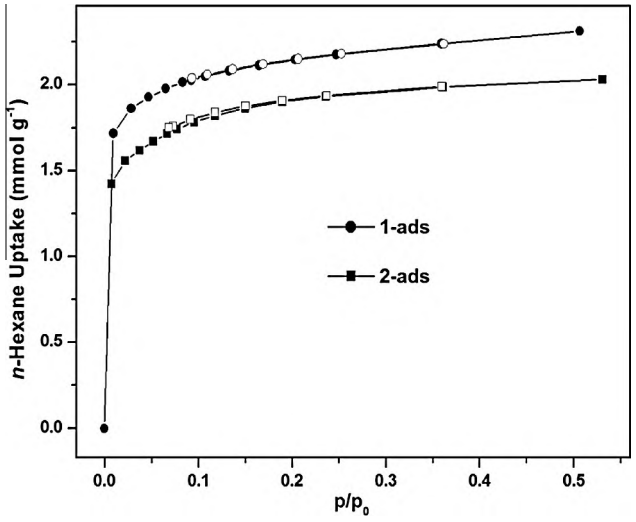

Fig. 7. *n*-Hexane adsorption (closed symbols) and desorption (open symbols) isotherms of thermally activated **1** (circles) and **2** (squares) measured at 50 °C.

Table 3
n-Hexane uptake values for **1**, **2**, MIL-47-F, Al-MIL-53-F, MIL-47 and Al-MIL-53 at 50 °C and $p/p_0 = 0.5$.

Compound	*n*-Hexane uptake (mmol g^{-1})
1	2.3
2	2.0
MIL-47-F [29]	2.3
Al-MIL-53-F [29]	2.3
MIL-47 [42]	2.0
Al-MIL-53 [41]	2.9

Thus, the increased hydrophobicity of **1**, achived through the incorporation of one additional –F group per linker as compared to MIL-47-F, helps it to adsorb the same amount of a hydrocarbon such as *n*-hexane, in spite of a noticiable difference in specific surace area between the two compounds.

4. Conclusions

Two new difluorinated MOFs, namely MIL-47-F_2 (**1**) and Al-MIL-53-F_2 (**2**) have been synthesized and characterized by a combination of different techniques such as XRPD analysis, DRIFT spectroscopy, thermogravimetric and elemental analysis. Compounds **1** and **2** are stable up to 340 and 480 °C, respectively, as revealed from the thermogravimetric analyses. As suggested by the N_2 and CO_2 sorption experiments, both **1** and **2** exhibit significant microporosity values, which are lower compared to their un-functionalized counterparts. From the single component adsorption isotherms, an ideal CO_2/N_2 selectivity value of 11 has been obtained for **2**. The breathing property of **2** upon adsorption of *n*-hexane is highly influenced due to fluorination, as compared to parent Al-MIL-53. High and low-pressure CO_2 sorption measurements confirm that the temperature region for the structural transition of **2** upon adsorption of CO_2 is lowered owing to fluorination, as compared to non-modified Al-MIL-53. The fluorination induces noticeable hydrophobicity to both of the difluorinated compounds, as demonstrated by the H_2O sorption experiments. Remarkably, at 50 °C and $p/p_0 = 0.5$, both mono- and difluorinated MIL-47 show high *n*-hexane uptake values, which surpass that of un-functionalized MIL-47 due to the enhanced hydrophobicity obtained via fluorination.

Acknowledgments

The authors would like to thank Mr. Geert Rampelberg of Department of Solid State Sciences, Ghent University, for assistance with the temperature-dependent XRPD measurements. This research is funded by Ghent University, GOA grant number 01G00710. CJ acknowledges funding by BMWi under grant 0327851A.

Appendix A. Supplementary data

Supplementary data associated with this article can be found, in the online version, at http://dx.doi.org/10.1016/j.micromeso.2013.07.030.

References

[1] G. Férey, Chem. Soc. Rev. 37 (2008) 191–214.
[2] S. Kitagawa, R. Kitaura, S. Noro, Angew. Chem. 116 (2004) 2388–2430; S. Kitagawa, R. Kitaura, S. Noro, Angew. Chem. Int. Ed. 43 (2004) 2334–2375.
[3] O.M. Yaghi, M. O'Keeffe, N.W. Ockwig, H.K. Chae, M. Eddaoudi, J. Kim, Nature 423 (2003) 705–714.
[4] L.J. Murray, M. Dincă, J.R. Long, Chem. Soc. Rev. 38 (2009) 1294–1314.
[5] J.-R. Li, R.J. Kuppler, H.-C. Zhou, Chem. Soc. Rev. 38 (2009) 1477–1504.
[6] L. Hamon, P.L. Llewellyn, T. Devic, A. Ghoufi, G. Clet, V. Guillerm, G.D. Pirngruber, G. Maurin, C. Serre, G. Driver, W. van Beek, E. Jolimaitre, A. Vimont, M. Daturi, G. Férey, J. Am. Chem. Soc. 131 (2009) 17490–17499.
[7] J. Lee, O.K. Farha, J. Roberts, K.A. Scheidt, S.T. Nguyen, J.T. Hupp, Chem. Soc. Rev. 38 (2009) 1450–1459.
[8] L. Ma, C. Abney, W. Lin, Chem. Soc. Rev. 38 (2009) 1248–1256.
[9] K.M.L. Taylor-Pashow, J. Della Rocca, Z.G. Xie, S. Tran, W.B. Lin, J. Am. Chem. Soc. 131 (2009) 14261–14263.
[10] P. Horcajada, T. Chalati, C. Serre, B. Gillet, C. Sebrie, T. Baati, J.F. Eubank, D. Heurtaux, P. Clayette, C. Kreuz, J.S. Chang, Y.K. Hwang, V. Marsaud, Y.-N. Bories, L. Cynober, S. Gil, G. Férey, P. Couvreur, R. Gref, Nat. Mater. 9 (2010) 172–178.
[11] M. Vallet-Regí, F. Balasm, D. Arcos, Angew. Chem. 119 (2007) 7692–7703; M. Vallet-Regí, F. Balasm, D. Arcos, Angew. Chem. Int. Ed. 46 (2007) 7548–7558.
[12] P. Horcajada, C. Serre, M. Vallet-Regi, M. Sebban, F. Taulelle, G. Férey, Angew. Chem. 118 (2006) 6120–6124; P. Horcajada, C. Serre, M. Vallet-Regi, M. Sebban, F. Taulelle, G. Férey, Angew. Chem. Int. Ed. 45 (2006) 5974–5978.
[13] G. Férey, C. Serre, Chem. Soc. Rev. 38 (2009) 1380–1399.
[14] K.K. Tanabe, S.M. Cohen, Chem. Soc. Rev. 40 (2011) 498–519.
[15] M. Eddaoudi, J. Kim, N. Rosi, D. Vodak, J. Wachter, M. O'Keefe, O.M. Yaghi, Science 295 (2002) 469–472.
[16] C. Yang, X.P. Wang, M.A. Omary, J. Am. Chem. Soc. 129 (2007) 15454–15455.
[17] S. Horike, S. Bureekaew, S. Kitagawa, Chem. Commun. (2008) 471–473.
[18] S.T. Meek, J.J. Perry IV, S.L. Teich-McGoldrick, J.A. Greathouse, M.D. Allendorf, Cryst. Growth Des. 11 (2011) 4309–4312.
[19] F. Debatin, K. Behrens, J. Weber, I.A. Baburin, A. Thomas, J. Schmidt, I. Senkovska, S. Kaskel, A. Kelling, N. Hedin, Z. Bacsik, S. Leoni, G. Seifert, C. Jäger, C. Günter, U. Schilde, A. Friedrich, H.-J. Holdt, Chem. Eur. J. 18 (2012) 11630–11640.
[20] A. Khutia, H.U. Rammelberg, T. Schmidt, S. Henninger, C. Janiak, Chem. Mater. 25 (2013) 790–798.
[21] I. Boldog, L. Xing, A. Schulz, C. Janiak, C. R. Chim. 15 (2012) 866–877.
[22] R. Custelcean, M.G. Gorbunova, J. Am. Chem. Soc. 127 (2005) 16362–16363.
[23] V. Colombo, C. Montoro, A. Maspero, G. Palmisano, N. Masciocchi, S. Galli, E. Barea, J.A.R. Navarro, J. Am. Chem. Soc. 134 (2012) 12830–12843.
[24] M. Kandiah, M.H. Nilsen, S. Usseglio, S. Jakobsen, U. Olsbye, M. Tilset, C. Larabi, E.A. Quadrelli, F. Bonino, K.P. Lillerud, Chem. Mater. 22 (2010) 6632–6640.
[25] S. Biswas, T. Ahnfeldt, N. Stock, Inorg. Chem. 50 (2011) 9518–9526.
[26] T. Devic, P. Horcajada, C. Serre, F. Salles, G. Maurin, B. Moulin, D. Heurtaux, G. Clet, A. Vimont, J.-M. Grenèche, B. Le Ouay, F. Moreau, E. Magnier, Y. Filinchuk, J. Marrot, J.-C. Lavalley, M. Daturi, G. Férey, J. Am. Chem. Soc. 132 (2010) 1127–1136.
[27] P. Horcajada, F. Salles, S. Wuttke, T. Devic, D. Heurtaux, G. Maurin, A. Vimont, M. Daturi, O. David, E. Magnier, N. Stock, Y. Filinchuk, D. Popov, C. Riekel, G. Férey, C. Serre, J. Am. Chem. Soc. 133 (2011) 17839–17847.
[28] T. Devic, F. Salles, S. Bourrelly, B. Moulin, G. Maurin, P. Horcajada, C. Serre, A. Vimont, J.-C. Lavalley, H. Leclerc, G. Clet, M. Daturi, P.L. Llewellyn, Y. Filinchuk, G. Férey, J. Mater. Chem. 22 (2012) 10266–10273.
[29] S. Biswas, T. Rémy, S. Couck, D. Denysenko, G. Rampelberg, J.F.M. Denayer, D. Volkmer, C. Detavernier, P. Van Der Voort, Phys. Chem. Chem. Phys. 15 (2013) 3552–3561.
[30] K. Barthelet, J. Marrot, D. Riou, G. Férey, Angew. Chem. 114 (2002) 291–294; K. Barthelet, J. Marrot, D. Riou, G. Férey, Angew. Chem. Int. Ed. 41 (2002) 281–284.
[31] T. Loiseau, C. Serre, C. Huguenard, G. Fink, F. Taulelle, M. Henry, T. Bataille, G. Férey, Chem. Eur. J. 10 (2004) 1373–1382.

[32] A. Boutin, F.-X. Coudert, M.-A. Springuel-Huet, A.V. Neimark, G. Férey, A.-H. Fuchs, J. Phys. Chem. C 114 (2010) 22237–22244.
[33] A. Boutin, S. Couck, F.-X. Coudert, P. Serra-Crespo, J. Gascon, F. Kapteijn, A.H. Fuchs, J.F.M. Denayer, Microporous Mesoporous Mater. 140 (2011) 108–113.
[34] S. Couck, J.F.M. Denayer, G.V. Baron, T. Rémy, J. Gascon, F. Kapteijn, J. Am. Chem. Soc. 131 (2009) 6326–6327.
[35] V. Finsy, L. Maa, L. Alaerts, D.E. De Vos, G.V. Baron, J.F.M. Denayer, Microporous Mesoporous Mater. 120 (2009) 221–227.
[36] E. Stavitski, E.A. Pidko, S. Couck, T. Rémy, E.J.M. Hensen, B.M. Weckhuysen, J.F.M. Denayer, J. Gascon, F. Kapteijn, Langmuir 27 (2011) 3970–3976.
[37] S. Bourrelly, P.L. Llewellyn, C. Serre, F. Millange, T. Loiseau, G. Férey, J. Am. Chem. Soc. 127 (2005) 13519–13521.
[38] P.L. Llewellyn, G. Maurin, T. Devic, S. Loera-Serna, N. Rosenbach, C. Serre, S. Bourrelly, P. Horcajada, Y. Filinchuk, G. Férey, J. Am. Chem. Soc. 130 (2008) 12808–12814.
[39] S. Couck, T. Rémy, G.V. Baron, J. Gascon, F. Kapteijn, J.F.M. Denayer, Phys. Chem. Chem. Phys. 12 (2010) 9413–9418.
[40] P.L. Llewellyn, P. Horcajada, G. Maurin, T. Devic, N. Rosenbach, S. Bourrelly, C. Serre, D. Vincent, S. Loera-Serna, Y. Filinchuk, G. Férey, J. Am. Chem. Soc. 131 (2009) 13002–13008.
[41] T.K. Trung, P. Trens, N. Tanchoux, S. Bourrelly, P.L. Llewellyn, S. Loera-Serna, C. Serre, T. Loiseau, F. Fajula, J. Am. Chem. Soc. 130 (2008) 16926–16932.
[42] T.K. Trung, I. Déroche, A. Rivera, Q. Yang, P. Yot, N. Ramsahye, S.D. Vinot, T. Devic, P. Horcajada, C. Serre, G. Maurin, P. Trens, Microporous Mesoporous Mater. 140 (2011) 114–119.
[43] N. Rosenbach Jr., A. Ghoufi, I. Déroche, P.L. Llewellyn, T. Devic, S. Bourrelly, C. Serre, G. Férey, G. Maurin, Phys. Chem. Chem. Phys. 12 (2010) 6428–6437.
[44] P.G. Yot, Q. Ma, J. Haines, Q. Yang, A. Ghoufi, Chem. Sci. 3 (2012) 1100–1104.
[45] C. Yang, X. Wang, M.A. Omary, J. Am. Chem. Soc. 129 (2007) 15454–15455.
[46] T. Wu, L. Shen, M. Luebbers, C. Hu, Q. Chen, Z. Ni, R.I. Masel, Chem. Commun. 46 (2010) 6120–6122.
[47] C. Yang, U. Kaipa, Q.Z. Mather, X. Wang, V. Nesterov, A.F. Venero, M.A. Omary, J. Am. Chem. Soc. 133 (2011) 18094–18097.
[48] H. Jasuja, Y. Huang, K.S. Walton, Langmuir 28 (2012) 16874–16880.
[49] H. Jasuja, N.C. Burtch, Y. Huang, Y. Cai, K.S. Walton, Langmuir 29 (2013) 633–642.
[50] D. Ma, Y. Li, Z. Li, Chem. Commun. 47 (2011) 7377–7379.
[51] C. Volkringer, D. Popov, T. Loiseau, G. Férey, M. Burghammer, C. Riekel, M. Haouas, F. Taulelle, Chem. Mater. 21 (2009) 5695–5697.
[52] T. Loiseau, L. Lecroq, C. Volkringer, J. Marrot, G. Férey, M. Haouas, F. Taulelle, S. Bourrelly, P.L. Llewellyn, M. Latroche, J. Am. Chem. Soc. 128 (2006) 10223–10230.
[53] C. Volkringer, D. Popov, T. Loiseau, N. Guillou, G. Férey, M. Haouas, F. Taulelle, C. Mellot-Draznieks, M. Burghammer, C. Riekel, Nat. Mater. 6 (2007) 760–764.
[54] J. Gascon, U. Aktay, M.D. Hernandez-Alonso, G.P.M. van Klink, F. Kaptejin, J. Catal. 261 (2009) 75–87.
[55] T. Ahnfeldt, D. Gunzelmann, T. Loiseau, D. Hirsemann, J. Senker, G. Férey, N. Stock, Inorg. Chem. 48 (2009) 3057–3064.
[56] D. Himsl, D. Wallacher, M. Hartmann, Angew. Chem. Int. Ed. 48 (2009) 4639–4642.
[57] C. Volkringer, T. Loiseau, N. Guillou, G. Férey, M. Haouas, F. Taulelle, E. Elkaim, N. Stock, Inorg. Chem. 49 (2010) 9852–9862.
[58] A. Comotti, S. Bracco, P. Sozzani, S. Horike, R. Matsuda, J. Chen, M. Takata, Y. Kubota, S. Kitagawa, J. Am. Chem. Soc. 130 (2008) 13664–13672.
[59] N. Reimer, B. Gil, B. Marszalek, N. Stock, CrystEngComm 14 (2012) 4119–4125.
[60] J.K. Lee, J.-H. Kim, Y.J. Kim, Bull. Korean Chem. Soc. 24 (2003) 1029–1031.
[61] X.-S. Huang, F.-L. Qing, J. Fluorine Chem. 129 (2008) 1076.
[62] V. Petricek, M. Dusek, L. Palatinus, The Crystallographic Computing System, Institute of Physics, Praha, Czech Republic, 2000.
[63] A. Centrone, T. Harada, S. Speakman, T.A. Hatton, Small 6 (2010) 1598–1602.
[64] H. Li, W. Shi, K. Zhao, Z. Niu, H. Li, P. Cheng, Chem. Eur. J. 19 (2013) 3358–3365.
[65] S.S. Nagarkar, A.K. Chaudhari, S.K. Ghosh, Inorg. Chem. 51 (2012) 572–576.
[66] S. Noro, Y. Hijikata, M. Inukai, T. Fukushima, S. Horike, M. Higuchi, S. Kitagawa, T. Akutagawa, T. Nakamura, Inorg. Chem. 52 (2013) 280–285.
[67] J. An, S.J. Geib, N.L. Rosi, J. Am. Chem. Soc. 132 (2010) 38–39.
[68] M. Majumder, P. Sheath, J.I. Mardel, T.G. Harvey, A.W. Thornton, A. Gonzago, D.F. Kennedy, I. Madsen, J.W. Taylor, D.R. Turner, M.R. Hill, Chem. Mater. 24 (2012) 4647–4652.
[69] L. Hou, W.-J. Shi, Y.-Y. Wang, Y. Guo, C. Jin, Q.-Z. Shi, Chem. Commun. 47 (2011) 5464–5466.
[70] S. Henke, R.A. Fischer, J. Am. Chem. Soc. 133 (2011) 2064–2067.
[71] T. Li, D.-L. Chen, J.E. Sullivan, M.T. Kozlowski, J.K. Johnson, N.L. Rosi, Chem. Sci. 4 (2013) 1746–1755.
[72] L. Du, Z. Lu, K. Zheng, J. Wang, X. Zheng, Y. Pan, X. You, J. Bai, J. Am. Chem. Soc. 135 (2013) 562–565.
[73] G.E. Cmarik, M. Kim, S.M. Cohen, K.S. Walton, Langmuir 28 (2012) 15606–15613.
[74] H. Wu, R.S. Reali, D.A. Smith, M.C. Trachtenberg, J. Li, Chem. Eur. J. 16 (2010) 13951–13954.
[75] J. Zhang, H. Wu, T.J. Emge, Jing Li, Chem. Commun. 46 (2010) 9152–9154.
[76] A.V. Neimark, F.-X. Coudert, A. Boutin, A.H. Fuchs, J. Phys. Chem. Lett. 1 (2010) 445–449.
[77] K.S.W. Sing, D.H. Everett, R.A.W. Haul, L. Moscou, R.A. Pierotti, J. Rouquerol, T. Siemieniewska, Pure Appl. Chem. 57 (1985) 603–619.
[78] S. Horike, D. Tanaka, K. Nakagawa, S. Kitagawa, Chem. Commun. (2007) 3395–3397.
[79] S. Paranthaman, F.-X. Coudert, A.H. Fuchs, Phys. Chem. Chem. Phys. 12 (2010) 8123–8129.